

Direct Georeferencing of Static Terrestrial Laser Scans

Jens-André PAFFENHOLZ and Hansjörg KUTTERER, Germany

Key words: engineering survey, laser scanning, positioning, direct georeferencing, static mapping, kinematic GPS

SUMMARY

This paper works on an adapted sensor-driven method for direct georeferencing of static terrestrial laser scans. The presented approach deals with the direct estimation of the sensor position with GPS antennas installed on the laser scanner. The advantage of this strategy is to use the constant rotation of the laser scanner with the combination of kinematic GPS measurements. Two major points are to be solved in direct georeferencing procedure: first the problem of the time synchronization of the laser scanner data and the position data and second the calculation of an azimuth for each scan line in the 3D laser scan from the GPS trajectory of the sensor. For this calculation a robust estimation of the required space curve is implemented to improve the results. First results with this improved estimation strategy are presented and also a comparison of different GPS solutions which provide the data basis of this method. The benefit of this direct georeferencing of terrestrial laser scans is a metric uncertainty of about 1 *cm* for the azimuth calculation on a distance of 30 *m*.

ZUSAMMENFASSUNG

In diesem Beitrag wird ein Verfahren zur direkten Georeferenzierung von statischen terrestrischen Laserscans vorgestellt. In dem vorgestellten Verfahren erfolgt die direkte Bestimmung der Sensorposition durch auf dem Laserscanner adaptierte GPS Antennen. Der Vorteil dieser Methode ist die Nutzung der konstanten Rotation des Laserscanners in Kombination mit kinematischem GPS. Zur direkten Georeferenzierung sind zwei wesentliche Schritte notwendig. In einem ersten Schritt ist die zeitliche Synchronisation zwischen den erfassten 3D-Laserscans und der kinematischen GPS-Trajektorie sicher zu stellen. Der zweite Schritt ist die eigentliche Berechnung eines Azimutes für jedes Profil des 3D-Laserscans aus der GPS-Trajektorie des Laserscanners. Hierzu wird eine robuste Schätzung der Trajektorie des Laserscanners durchgeführt, um somit die Ergebnisse für die Parameter der Raumkurve zu verbessern. Es werden erste Ergebnisse sowie ein Vergleich von verschiedenen GPS Lösungen, welche die Datengrundlage dieses Verfahren liefern, vorgestellt. Eine Gegenüberstellung mit terrestrischen Messungen zeigt das Potential dieses Verfahrens. Es ergeben sich für ausgewählte Objektkoordinaten aus der Unsicherheit der Azimutzuordnung metrische Abweichungen von 1 *cm* auf eine Entfernung von 30 *m*.

Direct Georeferencing of Static Terrestrial Laser Scans

Jens-André PAFFENHOLZ and Hansjörg KUTTERER, Germany

1 INTRODUCTION AND MOTIVATION

Nowadays several applications require 3D data. On the one hand there are 3D city models for planning issues or documentation tasks for example in forensics or architecture. On the other hand there are typical tasks of geodetic engineering like deformation measurements or precise documentation. In most of these cases the position of the 3D data is required in an absolute or global coordinate system, respectively. Terrestrial laser scanning is a very comfortable and often fast way to acquire 3D data in short ranges up to mid-ranges. The data acquisition of terrestrial laser scanners is done in a relative or local sensor-defined coordinate system, respectively. Hence the 3D point clouds have to be transformed to an absolute coordinate system. The required quality of the transformation depends on the application. The traditional method of georeferencing static terrestrial laser scans is to use control points. This is an indirect method which can be very time expensive. For example in geodetic engineering tasks, especially deformation measurements, an accuracy of a few millimeters is demanded.

An approach for acquiring 3D data in an efficient and effective way is called rapid mapping using kinematic terrestrial laser scanning (k-TLS). The main characteristics of k-TLS are fast high frequency reflectorless and immediate 3D data acquisition combined with a high spatial resolution for short ranges up to mid-ranges ($< 80\text{ m}$) with phase-based laser scanners (KUTTERER 2007).

k-TLS is divided in two variants: scanning from a moving platform of static objects (also known as mobile mapping) as well as fast scanning from a static platform (KUTTERER 2007). In mobile mapping applications georeferencing is an essential part; for further details see HESSE & KUTTERER (2007) as well as VENNEGEERTS ET AL. (2008). For the transfer of fast scanning results from a static platform to an absolute coordinate system or to link different scans georeferencing techniques described in Section 2 are used.

2 METHODS FOR GEOREFERENCING OF STATIC TERRESTRIAL LASER SCANS

This section starts with a brief overview about known techniques for georeferencing of static terrestrial laser scans. Afterwards a newly developed approach for direct georeferencing developed at the Geodetic Institute (GIH) of the Leibniz Universität Hannover with an adapted sensor-driven method is introduced.

In advance there are some comments concerning the term georeferencing. Often the term registration is used beside the term georeferencing. Registration primarily indicates the linking of laser scans from different laser scanner stations. However in commercial software registration includes often both the linking of laser scans from different stations and the

transformation to a global coordinate system. In this paper the term registration is used to describe the linking of laser scans from different laser scanner stations. The term georeferencing is understood as transformation of the laser scans from the relative or local sensor system to an absolute or global system, respectively.

2.1 Brief overview about indirect, direct and data-driven basic approaches

The task of georeferencing of terrestrial 3D laser scans is to be solved if an absolute coordinate system is required for further data processing. There are several applications where georeferenced data are required as mentioned in Section 1. From the point of view of a geodetic engineer this is high-precise as-built documentation of objects with a broad range of geometric complexity. Also the inter-epochal comparison of laser scans and derived parameters for deformation monitoring applications require high-precise georeferenced data.

For estimating the transformation parameters between the local sensor system and an absolute coordinate system mainly three different approaches are known; for some further details see SCHUHMACHER & BÖHM (2005). The first approach is the *indirect method* which describes the traditional way of georeferencing in static terrestrial laser scanning applications. With the scanning of control points with known coordinates a geodetic datum is transferred to the point clouds. This method is more precise than the following two methods. But the determination of the control points coordinates with an independent surveying technique (e. g. tachymetry) is a complex and time-consuming task. Additionally the control points could be used as homologous points for registration of laser scans.

The second approach is the *direct method* which uses additional sensors, like navigation sensors, total stations or inclination sensors, to estimate directly the laser scanner position and orientation. Roughly speaking the additional sensors observe the transformation parameters between the relative sensor system and the absolute coordinate system. The benefit of this method is the immediate availability of the sensor position and orientation. By using additional sensors a complex sensor system is formed. Such a complex sensor system is already known from mobile mapping systems. The major point to solve is the time synchronization of the laser scanner and the additional sensors. The accuracy of this method depends on the quality of the delivered position and orientation information of the additional sensors. If the accuracy of the additional sensors does not allow estimating reliable transformation parameters for transferring the laser scans from the local sensor system to an absolute system the direct method can also be used to get start values for iterative algorithms for registration tasks, like the Iterative Closest Point (ICP) algorithm (PFEIFER ET AL. 2007).

The third approach is a *data-driven method* which uses a georeferenced data base and iterative algorithms like the ICP-algorithm to transform from the local sensor system to a global coordinate system. Because of the need of a georeferenced data base which affects the accuracy of the transformation this method is only mentioned to complete the brief overview about methods for georeferencing static terrestrial laser scans.

2.2 Newly developed approach for a direct georeferencing method

In this section the adapted sensor-driven method for direct georeferencing of terrestrial laser scans newly developed at the Geodetic Institute of the Leibniz Universität Hannover shall be presented. The aim of this approach is to use a minimized number of additional sensors to directly estimate the laser scanner position and orientation as briefly described in Section 2.1.

This approach works without traditionally georeferenced control points. And the operation of the laser scanner should not be disturbed. Caused by the high frequency data acquisition rate of a phase-based laser scanner the additional sensors should provide data with a rate of at least 10 Hz. Finally the constant rotation about the vertical axis of a phase-based laser scanner shall be used as time and orientation reference in the data acquisition process.

The above described aim can be achieved by kinematic GPS. A maximum number of two antennas are suitable to get the position and orientation of the laser scanner. The flexibility of the laser scanner is not disturbed. And also a high-frequency data acquisition and time synchronization of this hybrid sensor system is possible (HESSE & KUTTERER 2007).

The present realization of this hybrid sensor system at the Geodetic Institute is composed of a phase-based laser scanner which operates in normal 3D mode and provides 3D point clouds of the outdoor environment. The orbital motion of the laser scanner is observed by two geodetic L1/L2 GNSS receivers at 10 Hz data rate with antennas installed on top of the laser scanner. To obtain precise 3D positions for the orbital motion of the laser scanner and the additional transformation to an absolute coordinate system a GPS reference station is required (for example from the *German reference station network SAPOS*). The time synchronization for this hybrid sensor system can be provided by two different techniques: technique (a) is to use an external real-time process computer and technique (b) is to use the event marker input of the GNSS receiver.

For directly georeferencing the 3D laser scan an azimuth for each scan line is calculated. The trajectory of the antenna reference point (ARP) described by the orbital motion of the laser scanner is a space curve. This space curve is robustly estimated from the GPS trajectory.

3 DATA ACQUISITION AND PREPROCESSING

3.1 Data acquisition

The acquisition of the laser scans has been carried out with the *Leica HDS 4500* (also known as *Zoller+Fröhlich (Z+F) Imager 5003*) in normal 3D mode at three different stations. “*high, low noise*” have been used as scan parameters for horizontal positions from 0° up to 360° so that the recording time was approximately 15 minutes per station. To obtain the 3D positions for the orbital motion of the laser scanner the following GNSS equipment was used: One *Trimble 5700* receiver with *Geodetic Zephyr antenna* (left antenna in figure 3-1). This receiver has operated with 10 Hz data rate. It has additionally stored the ttl-impulses in the RINEX observation file. And one *Leica GRX1200GG Pro* receiver with *AX1202GG antenna* was used (right antenna in figure 3-1). This receiver has operated with 20 Hz data rate. In

addition one further *Leica GRX1200GG Pro* receiver was used as local reference station. It has also operated with 20 Hz data rate.



Figure 3-1: System setup for the measurements on 5th March 2008 in the “Ehrenhof” in the “Große Garten” of the “Herrenhäuser Gärten” in Hannover

3.2 Time synchronization

The captured static 3D laser scan consists of several scan lines which are characterized by one turn of the vertical step motor of the laser scanner. Per scan line one transistor-transistor-logic (ttl)-impulse is available which will be used for the time synchronization. To acquire the ttl-impulses the two techniques are available which have been briefly described in Section 2.2. For the actual system setup on 5th March 2008 the event marker input of the GPS receiver was used (technique (b)). As result a GPS timestamp for every ttl-impulse is obtained. An evaluation of this technique concerning the capabilities and limits in processing the high-frequency ttl-impulses from the laser scanner with the event marker input is given in PAFFENHOLZ & KUTTERER (2008).

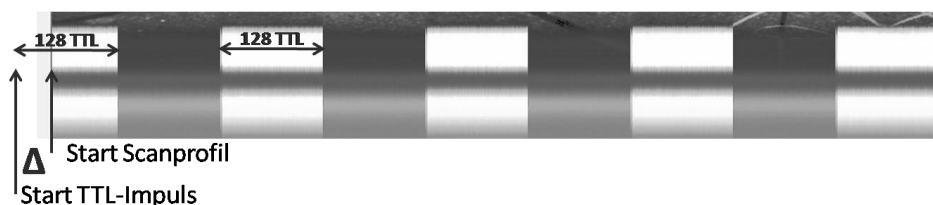


Figure 3-2: Detail of the ttl-impulses mapped in the laser scan as bright-dark change

For the data – laser scan and ttl-impulses – captured by the laser scanner some preprocessing is necessary. There is a production-caused latency period between the starting of data storage of the laser scan and of the registered ttl-impulses. Due to this latency period a smaller number of scan lines compared to registered ttl-impulses is captured. To solve this problem the ttl-impulses are mapped by a marker in the laser scan as bright-dark change (figure 3-2). This marker which changes from bright to dark in a defined impulse interval allows determining the latency period. After correcting the latency period and an optional

interpolation of missing ttl-impulses a unique synchronization between scan lines and ttl-impulses is possible.

3.3 GPS analysis

The GPS analysis was processed for the two antennas individually. The kinematic trajectory was processed with a local reference station in a distance of approximately 40 m to the laser scanner. The GPS analysis for the measurements with 10 Hz data rate produces about 8000 3D positions for the orbital motion of the laser scanner.

Two different software products were used for the GPS analysis: The software *Trimble Total Control (TTC) 2.73* which provides only variances for each 3D position, and the *Geodetic NAVSTAR Positioning (GEONAP)* software of the company *Geo++* which has the advantage that one gets a full variance-covariance matrix for each 3D position. Additionally a documentation of relevant adjustment results, such as the estimated variance factor, is available.

A comparison with a detailed evaluation of the GPS analysis by different software products will be given in future works. In this paper only the results of the direct georeferencing are compared – exactly the azimuth determination for each scan line – which are obtained by the GPS analysis of the two software products.

4 ROBUST ESTIMATION OF THE SPACE CURVE

The orbital trajectory of the ARP is caused by the rotation of the laser scanner about its vertical axis. This trajectory describes an orbital space curve. For the further processing the parameters center point and radius and also the adjusted observations have to be estimated. In the present state of work each GPS antenna was treated separately. An integrated analysis is in preparation.

This section deals with the two step model of the robust parameter estimation independent of the coordinate system. Nevertheless, for the further analysis a transformation to the Gauss-Krüger system has been performed to compare the results with terrestrial measurements by a tachymeter. The transformation was carried out for the 3D positions including variances and if available correlations with a tool of the GEONAP software for the two GPS analysis.

In the preceding approach in PAFFENHOLZ & KUTTERER (2008) the estimation was reduced to a two-dimensional problem because the space curve in the Gauss-Krüger system is sufficiently plane. To improve the results for the azimuth determination a two step model which allows robust parameter estimation was developed. The first step is the projection of the 3D positions onto a best-fitting plane. This step is required to take into account the full 3D information of the points. By this newly developed approach also rotations due to the coordinate transformations are respected. The second step is the estimation of a best-fitting circle through the projected positions. This step is necessary to directly improve the azimuth determination by using the adjusted observations instead of the original positions. The

advantage of this step over the earlier approach is that the space curve is better described by the adjusted positions than the original ones. This is because the noisy GPS positions are smoothed and in addition outlier detection could be performed.

In this newly developed approach the parameters of the best-fitting plane as well as the best-fitting circle are estimated in a least-squares adjustment. Robustness means here in this approach to perform Baarda's data-snooping for outlier detection and elimination.

4.1 Projection of the 3D positions onto a best-fitting plane

In the first step the 3D positions are orthogonally projected onto a best-fitting plane with a principal axis transformation following an algorithm published by DRIXLER (1993).

A 3D plane is given by $n_x \cdot x_i + n_y \cdot y_i + n_z \cdot z_i + d = 0$ with $\mathbf{n} = [n_x \quad n_y \quad n_z]^T$ the normal unit vector. The estimation of the 3D plane through the 3D positions of the orbital space curve starts with introducing centered point coordinates $\bar{\mathbf{x}}_i = \mathbf{x}_i - \mathbf{x}_S = \mathbf{x}_i - \frac{1}{k} \cdot \sum_{i=1}^k \mathbf{x}_i$ for every point $\mathbf{x}_i = [x_i \quad y_i \quad z_i]^T$ of the k positions in order to eliminate the distance parameter d .

The eigenvectors required for the principal axis transformation can be derived by an eigenvalue decomposition of the matrix

$$\mathbf{A} = \begin{bmatrix} \sum \bar{x}_i \cdot \bar{x}_i & \sum \bar{x}_i \cdot \bar{y}_i & \sum \bar{x}_i \cdot \bar{z}_i \\ \sum \bar{x}_i \cdot \bar{y}_i & \sum \bar{y}_i \cdot \bar{y}_i & \sum \bar{y}_i \cdot \bar{z}_i \\ \sum \bar{x}_i \cdot \bar{z}_i & \sum \bar{y}_i \cdot \bar{z}_i & \sum \bar{z}_i \cdot \bar{z}_i \end{bmatrix}. \quad (3.1)$$

The normal unit vector \mathbf{n} is given by the eigenvector associated with the minimal eigenvalue.

By use of the principal axis transformation the 3D positions $\mathbf{x}_i = [x_i \quad y_i \quad z_i]^T$ are transferred to the plane positions $\mathbf{u}_i = [u_i \quad v_i \quad w_i]^T$. This transformation leads to $w_i = 0$ for the third component.

To eliminate outliers in this first model step and to increase the robustness the perpendicular distances $v_{p,i}$ for all points are analyzed. Therefore a test value for each perpendicular distance is calculated and compared to the $(1-\alpha)$ quantile value of the normal distribution with a significance level $\alpha = 1\%$:

$$\frac{v_{p,i}}{\sigma_{v_p}} > N(0,1) \Rightarrow \text{reject } H_0. \quad (3.2)$$

All test values greater than the quantile value are considered as outliers. The corresponding points are eliminated in an iterative process.

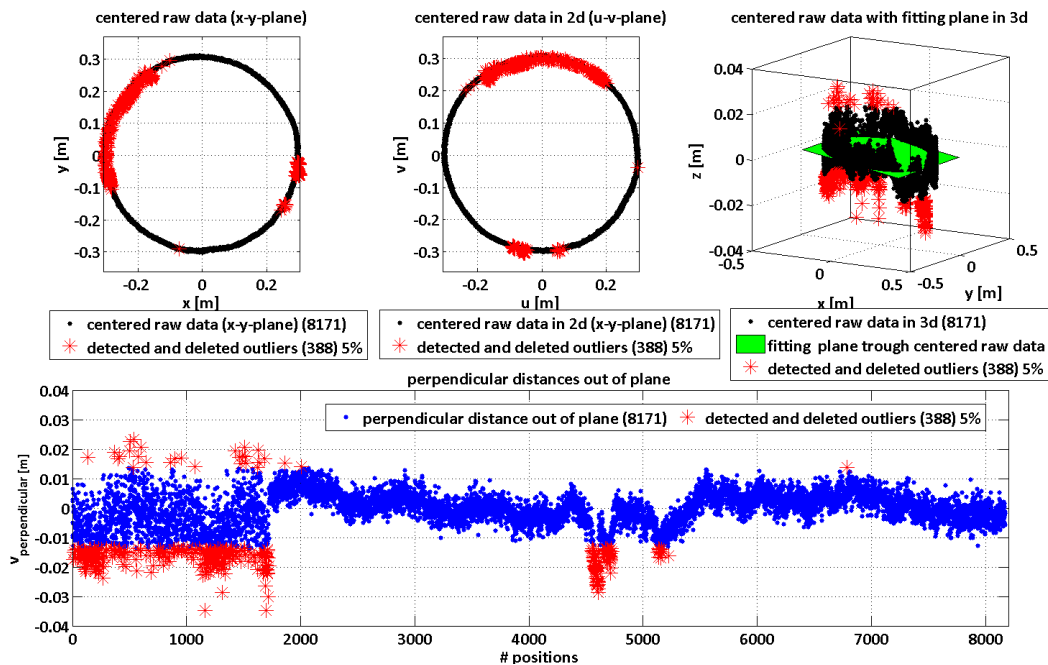


Figure 4-1: results of robust plane adjustment, GPS analysis with GEONAP

Figure 4-1 shows the result of the robust plane adjustment with the above described algorithm for one selected dataset. The positions are given in black color. Detected as well as deleted outliers according to equation (3.2) are given in red color. In the upper left sub-figure the original centered positions in the x-y-plane are presented. In the middle sub-figure one can see the result of the principal axis transformation in the u-v-plane system. The sub-figure in the upper right presents the best-fitting plane given in green color with the centered positions as well as outliers. At the bottom of figure 4-1 the perpendicular distance out of plane in blue color as well as detected and deleted outliers are presented. The high number of outliers concentrated at the beginning positions are possibly caused by shadowing effects. In detail this will be analyzed in further works.

As result for the first step – the projection of the 3D positions onto a best-fitting plane – one gets the input data for the second step.

4.2 Estimation of a best-fitting circle through the projected positions

In the second step the robust circle adjustment through the projected positions will be processed. Therefore the Gauss-Helmert model (GHM) is transformed into an equivalent Gauss-Markov model (GMM) to use the known data-snooping method for outlier detection. Compared with the plane adjustment the circle adjustment accounts for the stochastic information of the positions. The transformation from the GHM $\mathbf{f}(\hat{\mathbf{i}}, \hat{\mathbf{x}}) = \mathbf{0}$ into an equivalent GMM $\mathbf{f}(\hat{\mathbf{i}}_1, \hat{\mathbf{i}}_2, \hat{\mathbf{x}}) = \mathbf{0}$ is done according to JÄGER ET AL. (2005).

This approach by JÄGER ET AL. (2005) deals with a partitioning of the observations vector $\hat{\mathbf{I}}$ into $\hat{\mathbf{I}}_1$ and $\hat{\mathbf{I}}_2$. The part $\hat{\mathbf{I}}_2$ is treated beside the parameters $\hat{\mathbf{x}}$ as additional parameter group $\hat{\mathbf{y}}$. To correct the GHM the additional parameter group $\hat{\mathbf{y}}$ has to be introduced as direct observations group $\hat{\mathbf{I}}_2$. The linearized functional model as well as the stochastic model is then given by

$$\begin{bmatrix} -\mathbf{B}_1^{-1} \cdot \mathbf{A}_y & -\mathbf{B}_1^{-1} \cdot \mathbf{A} \\ \mathbf{I} & \mathbf{0} \end{bmatrix} \cdot \begin{bmatrix} d\hat{\mathbf{y}} \\ d\hat{\mathbf{x}} \end{bmatrix} + \begin{bmatrix} -\mathbf{B}_1^{-1} \cdot (\mathbf{l}_1, \mathbf{y}_0, \mathbf{x}_0) \\ \mathbf{0} \end{bmatrix} - \begin{bmatrix} \mathbf{v}_1 \\ \mathbf{v}_2 \end{bmatrix} = \mathbf{0}$$

$$\boldsymbol{\Sigma}_{ll} = \begin{bmatrix} \boldsymbol{\Sigma}_{ll,1} & \boldsymbol{\Sigma}_{l2,1} \\ \boldsymbol{\Sigma}_{2l,1} & \boldsymbol{\Sigma}_{ll,2} \end{bmatrix} = \sigma_0^2 \cdot \mathbf{P}^{-1} \quad (3.3)$$

with $\mathbf{B}_1 = \left(\frac{\partial \mathbf{f}}{\partial \mathbf{l}_1} \right)_{\mathbf{l}_1}$, $\mathbf{A}_y = \left(\frac{\partial \mathbf{f}}{\partial \hat{\mathbf{y}}} \right)_{\mathbf{l}, \mathbf{y}_0}$ and $\mathbf{A} = \left(\frac{\partial \mathbf{f}}{\partial \hat{\mathbf{x}}} \right)_{\mathbf{l}, \mathbf{x}_0}$

For the circle adjustment in the second step the position component u_i is introduced as $\hat{\mathbf{I}}_1$ and the position component v_i is introduced as $\hat{\mathbf{I}}_2$. The variance-covariance matrix $\boldsymbol{\Sigma}_{ll}$ is given by the GPS analysis. Stochastic information is given for every position. Correlations between the positions are not available. As variance factor σ_0^2 the estimated variance factor of the GPS analysis is introduced. If this value is not available $\sigma_0^2 = 1$ is set.

To eliminate outliers in this second model step and to increase the robustness the parameter estimation according to equation (3.3) is done iteratively. For each position \mathbf{u}_i a test value is calculated and compared to the $(1-\alpha)$ quantile value of the Fisher distribution with a significance level $\alpha = \frac{5\%}{r}$, with r the redundancy of the model. In every iteration step the position with the largest test value greater than the quantile value is rejected.

After the parameter estimation is finished the adjusted positions and the center point are transformed by the principal axis transformation to the original x-y-z-coordinate system.

Figure 4-2 shows the results of the robust circle adjustment. In all sub-figures the input data are given in black color, the adjustment results are given in green color and the detected as well as deleted outliers are given in red color. In the upper left sub-figure the adjusted positions are presented in u-v-plane. The sub-figure in the middle presents the final result of the two step model for robust estimation of the space curve with equal axis scaling. The upper right sub-figure presents again the final adjustment result with a different scaling for the height component to better show the height variation of the GPS positions. The sub-figure at the bottom shows the range of variation in radius for the estimated positions. In comparison with the construction value of the GPS antenna adaption the estimated radius with 0.300 m fits in a range of a few 10th millimeters.

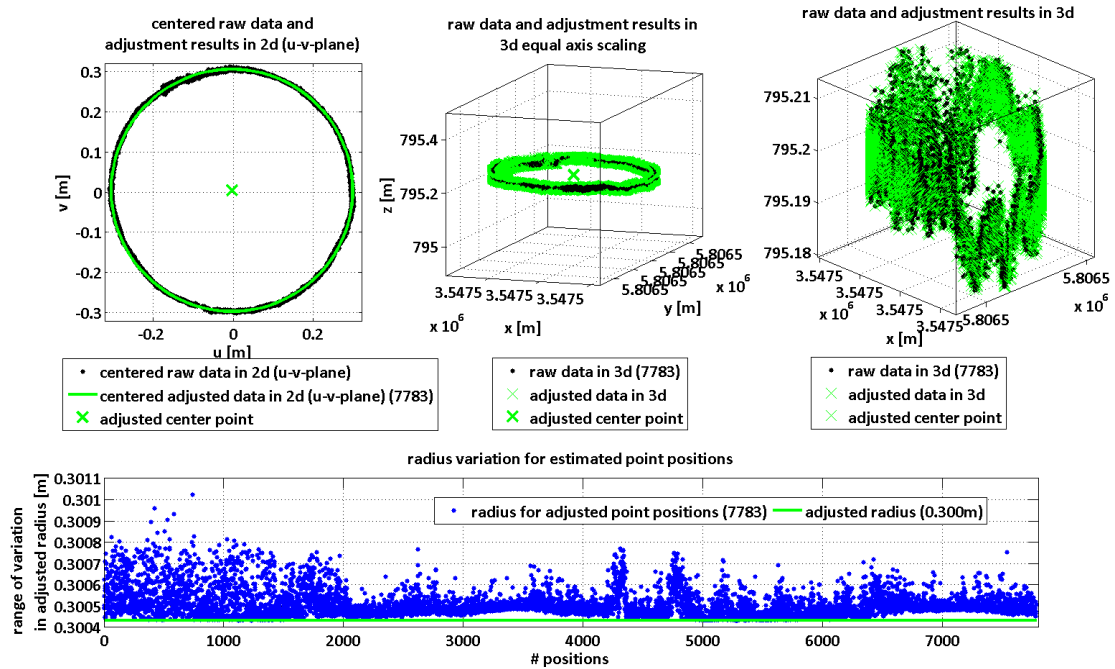


Figure 4-2: results of robust circle adjustment, GPS analysis with GEONAP

A short wrap-up for the robust estimation of the space curve: The input data were about 8000 positions in a global coordinate system (here Gauss-Krüger). During the first step – the projection of the 3D positions onto a best-fitting plane – all points which were detected as outliers according to equation (3.2) were deleted. For the presented dataset these were 5 % of the whole positions. During the second step – the estimation of a best-fitting circle through the projected positions – all projected points which were detected as outliers according to equation (3.3) were deleted. Actually, for this dataset no projected positions were deleted. Finally the adjustment results were transformed to the original x-y-z-coordinate system.

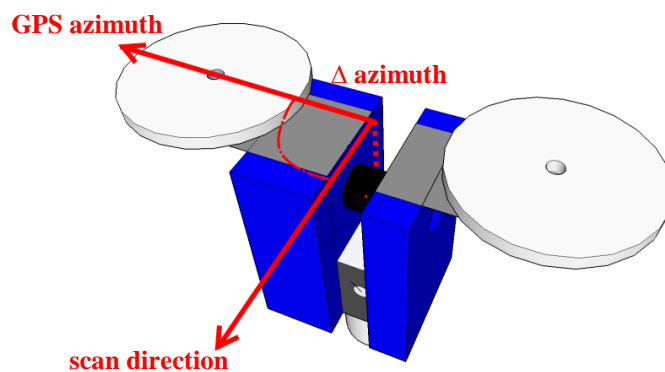


Figure 4-3: Schematic representation of the Δ azimuth

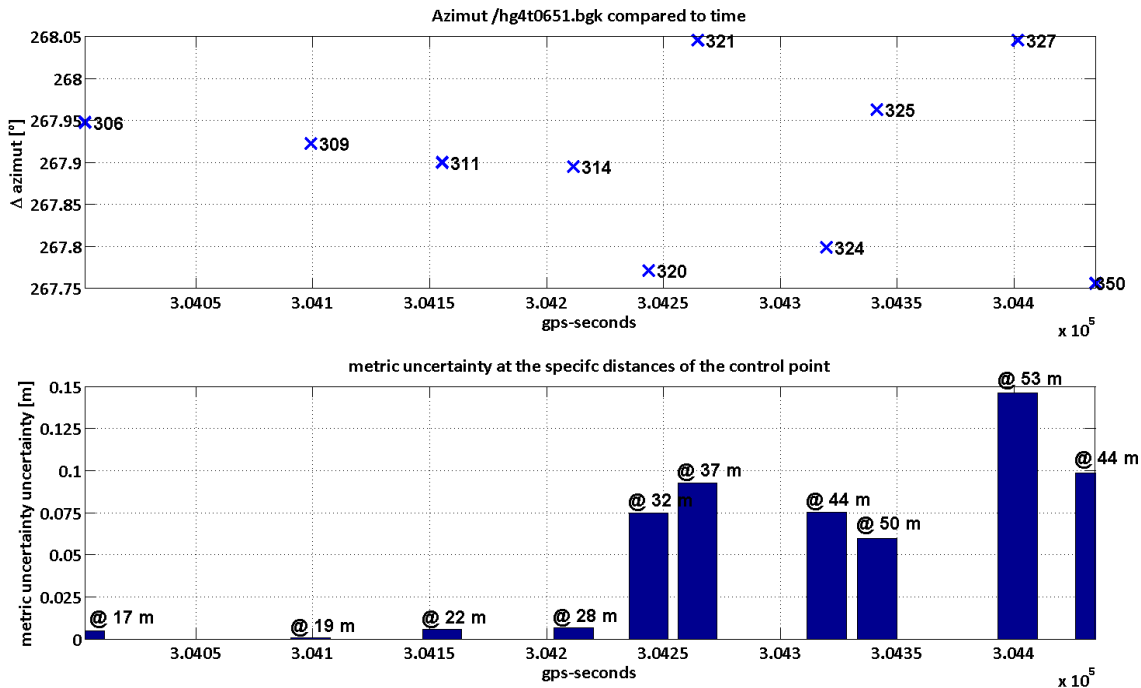


Figure 4-4: Δ azimuth for a choice of scan lines over time, GPS analysis with GEONAP

5 AZIMUTH DETERMINATION AND RESULT VALIDATION

As last step to get a directly georeferenced static terrestrial laser scan an azimuth for each scan line has to be determined. Therefore the arrangement of the GPS antennas at the laser scanner has to be considered (cf. figure 4-3). For this arrangement of the GPS antennas in relation to the scan direction an offset, Δ azimuth, between the scan line and the corresponding part of the GPS trajectory exists. The value for Δ azimuth can be derived by the constant rotation of the laser scanner about its vertical axis. Δ azimuth is constant if it is not affected by any faults.

In the performed field check the Δ azimuth was determined from the measurements. For evaluation purposes tachymeter measurements for selected control points were additionally done. The comparison of the tachymeter direction with the laser scanner direction in the selected control points (Δ azimuth) is presented in top of figure 4-4. Assuming that the rotation of the laser scanner is constant the Δ azimuth over the time should be a horizontal line. The range of variation in distances to a linear regression is about 0.29° . For a rating of these distances the corresponding distances from the laser scanner to the control points have to be considered. This is done in the bottom of figure 4-4 where the metric uncertainty at the specific distance of the control point is presented. One can see that for short distances up to 30 m (control points: 306, 309, 311 and 314) the metric uncertainty is about 5 cm. For mid-distances about 30 m to 50 m (control points: 320, 321, 324, 325, 327 and 350) the metric uncertainty is about 10 cm. But here the maximum range of the used laser

scanner (53 m) has to be respected. Nevertheless the results show that the presented approach has a great potential for direct georeferencing of static terrestrial laser scans in typical ranges up to 30 m for the used laser scanner *Leica HDS 4500*.

Table 5-1: Comparison of azimuth determination results obtained by GEONAP and TTC

	hg4_trimble	hg4_leica	Dataset	hg4_trimble	hg4_leica	
GEONAP	388 8171	1166 15926	# outliers plane # positions plane	452 8037	763 15695	TTC
	$x = 483.134$ $y = 468.194$ $z = 795.197$	$x = 483.135$ $y = 468.193$ $z = 795.205$	Center point [m]	$x = 483.134$ $y = 468.191$ $z = 795.171$	$x = 483.135$ $y = 468.191$ $z = 795.193$	
	$r = 0.300$	$r = 0.304$	Radius [m]	$r = 0.299$	$r = 0.305$	
	0 7783	0 7380	# outliers circle # positions circle	134 7585	157 7448	
	0.10	0.10	$\sigma_{\Delta \text{azimuth}} [^\circ]$	0.17	0.10	
	0.04	0.04	Max metric avg uncertainty @ 25 m [m]	0.07	0.04	

Table 5-1 shows a comparison of azimuth determination results obtained with the two software products introduced in Section 3.3. The displayed dataset is captured from the red marked station in figure 5-1. Table 5-1 contains the results for the two on the laser scanner adapted antennas. As already mentioned the GPS analysis is done separately for the antennas at the moment. One comment to the “_leica” named antennas: In the robust circle adjustment only half of the positions could be processed. This is caused by memory limitations of the normal desktop computer in calculation, regarding the great dimensions of matrices in the adjustment.



Figure 5-1: Scene on 5th March 2008 in the “Ehrenhof” in the “Große Garten” of the “Herrenhäuser Gärten” in Hannover

The values for the estimated center point are nearly identical except for the height component. This difference can be explained by possibly different settings for the antenna corrections and heights in the GPS analysis software. The radius varies in a range of a few millimeters. It also fits in a range of a few millimeters to the construction value of the GPS antenna adaption. The

number of outliers for all done estimations is in maximum about 5 %. This is acceptable. The standard deviation $\sigma_{\Delta \text{azimuth}}$ varies about 0.07° for the four datasets. The maximum metric average uncertainty at a distance of 25 m is for all shown data in an acceptable range.

6 ERROR BUDGET OF THE METHOD FOR DIRECT GEOREFERENCING OF STATIC TERRESTRIAL LASER SCANS

In this section the error budget of the presented newly developed approach for direct georeferencing of static terrestrial laser scans is discussed. Therefore the components of the hybrid sensors system have to be considered separately.

The laser scanner captures 3D point clouds of the outdoor environment. Because it is a polar measuring system the measurements are affected by typical errors well known from polar measuring system. Nevertheless we want to concentrate here only on that kind of errors directly concerning the presented approach. One possible error could be a trunnion axis error caused by the weight of the antennas. Another one could be an anomaly in the rotation speed.

The GNSS component as well as the GPS analysis plays a central in the presented approach. The mentioned errors are again directly concerning the presented approach. One problem might be the near-field effect caused by the antenna adaption made of aluminum on the laser scanner or possibly multipath. The alternating antenna orientation could affect another error. Therefore a solution could be to introduce elevation dependent phase center variations.

In further work the briefly described error budget will be focused on. On the one hand practical measurements and on the other hand theoretical analysis will be performed.

7 CONCLUSIONS AND FUTURE WORK

This paper presents an adapted sensor-driven method for direct georeferencing of static terrestrial laser scans. The presented newly developed approach deals with the direct estimation of the sensor position with GPS antennas installed on the laser scanner. The constant rotation of the laser scanner is used in combination with kinematic GPS measurements in this strategy. After solving the time synchronization a two step model for robust estimation of the space curve of the ARP caused by the orbital motion of the laser scanner was implemented. The presented results show the potential of this method. This is a metric uncertainty of about 1 cm for the azimuth calculation on a distance of 30 m .

Future work will focus on an integrated analysis of the two GPS antennas. Also the stochastic information should be considered for the plane adjustment to improve the first step of the robust estimation of the space curve. Further on the presented direct georeferencing procedure should be used with the Z+F Imager 5006. Due to the technical specifications of this laser scanner a further enhancement of the direct georeferencing procedure is to be expected. Also future work will concentrate on a better understanding and reduction of the presented error budget.

ACKNOWLEDGEMENTS

The authors would like to thank Dipl.-Ing. Frank Hinsche from *Leica Geosystems* who has provided two *Leica GPS1200GX Pro* equipments. Also thanks are given to Vincent Meiser for the support during the data acquisition.

REFERENCES

- Drixler, E. (1993): *Analyse der Form und Lage von Objekten im Raum*. Deutsche Geodätische Kommission (DGK) : Reihe C, Dissertationen; Heft Nr. 409, München
- Hesse, C. & Kutterer H. (2007): *A Mobile Mapping System using Kinematic Terrestrial Laser Scanning (KTLS) for Image Acquisition*. In: Grün, A. & Kahmen, H. (Eds.): *Optical 3-D Measurement Techniques VIII (Vol. II)*, ETH Zürich, pp. 134-141
- Kutterer, H. (2007): *Kinematisches terrestrisches Laserscanning – Stand und Potenziale*. In: Luhmann, T. & Müller, C. (Hrsg.): *Photogrammetrie - Laserscanning - Optische 3D-Messtechnik*, Beiträge der Oldenburger 3D-Tage 2007, Verlag Herbert Wichmann, Heidelberg, S. 2-9
- Jäger, R., Müller, T., Saler, H. & Schwäble, R. (2005): *Klassische und robuste Ausgleichungsverfahren*, Kapitel Standards und Erweiterungen in der Ausgleichung nach der Methode der kleinsten Quadrate (L2-Norm), Verlag Herbert Wichmann, Heidelberg, S. 144-236
- Paffenholz, J.-A. & Kutterer, H. (2008): *Ein Verfahren zur schnellen statischen Georeferenzierung von 3D-Laserscans*. In: Luhmann, T. und Müller, C. (Hrsg.): *Photogrammetrie - Laserscanning - Optische 3D-Messtechnik*, Beiträge der Oldenburger 3D-Tage 2008, Verlag Herbert Wichmann, 2008. In Vorbereitung.
- Pfeifer, N., Haring, A. & Briese, C. (2007): *Automatische Auswertung im terrestrischen Laserscanning*. In: *Terrestrisches Laserscanning (TLS 2007) Ein Messverfahren erobert den Raum* (74. DVW-Seminar), Schriftenreihe des DVW Band 53, S. 43-57
- Schuhmacher, S. & Böhm, J. (2005): *Georeferencing of terrestrial laser scanner data for applications in architectural modeling*. In *3D-ARCH 2005: Virtual Reconstruction and Visualization of Complex Architectures*, volume XXXVI, PART 5/W17 of International Archives of Photogrammetry, Remote Sensing and Spatial Information Sciences
- Vennegeerts, H., Martin, J., Becker, M. & Kutterer, H. (2008): *Validation of a Kinematic Laserscanning System*. In: *Journal of Applied Geodesy*, (in print)

BIOGRAPHICAL NOTES

Prof. Dr. Hansjörg Kutterer received his Dipl.-Ing. and Ph.D. in Geodesy at the University of Karlsruhe in 1990 and 1993, respectively. Since 2004 he is a Full Professor at the Geodetic Institute of the Leibniz Universität of Hannover. His research areas are: adjustment theory and

TS 1H – Developments in Scanner and Sensor Technologies

14/15

Jens-André Paffenholz and Hansjörg Kutterer

Direct Georeferencing of Static Terrestrial Laser Scans (2776)

Integrating the Generations

FIG Working Week 2008

Stockholm, Sweden 14-19 June 2008

error models, quality assessment, geodetic monitoring, terrestrial laser scanning and automation of measurement processes. He is active in national and international scientific associations and designated Vice President of the Deutscher Verein für Vermessungswesen e.V. (DVW). In addition he is member of the editorial board of the Journal of Applied Geodesy.

Jens-André Paffenholz received his Dipl.-Ing. in Geodesy and Geoinformatics at the Leibniz Universität Hannover in 2006. Since 2006 he is research assistant at the Geodetic Institute at the Leibniz Universität Hannover. His main research interests are: terrestrial laser scanning, industrial measurement system, automation of measurement processes and robot calibrations. He is member in the Working Group WG 4.2.3: “Application of Artificial Intelligence in Engineering Geodesy” of IAG Commission 4 (Positioning and Applications).

CONTACTS

Jens-André Paffenholz
Geodätisches Institut
Leibniz Universität Hannover
Nienburger Str. 1
30167 Hannover
GERMANY
Tel. +49 511 762 3191
Fax + 49 511 762 2468
Email: paffenholz@gih.uni-hannover.de
Webpage: www.gih.uni-hannover.de

Prof. Dr. Hansjörg Kutterer
Geodätisches Institut
Leibniz Universität Hannover
Nienburger Str. 1
30167 Hannover
GERMANY
Tel. +49 511 762 2461
Fax + 49 511 762 2468
Email: kutterer@gih.uni-hannover.de
Webpage: www.gih.uni-hannover.de